EFFECTS OF STRAIN-INDUCED DEFECTS ON EXCESS CARRIER LIFETIME AND AMBIPOLAR DIFFUSION IN *nipi*-DOPED $In_{0.2}Ga_{0.8}As$/GaAs MQWs

H.T. LIN,* D.H. RICH,* AND A. LARSSON**
*Department of Materials Science & Engineering, University of Southern California, Los Angeles, CA 90089-0241
**Department of Optoelectronics and Electrical Measurements, Chalmers University of Technology, S-412 96 Göteborg, Sweden

ABSTRACT

The effects of strain-induced defects on excess carrier lifetime and transport in a *nipi*-doped $In_{0.2}Ga_{0.8}As$/GaAs multiple quantum well (MQW) structure were examined with a new method called *electron beam-induced absorption modulation* (EBIA) in which the kinetics of carrier transport and recombination are examined with a high-spatial, -spectral and -temporal resolution. The excess carrier lifetime and ambipolar diffusion were found to be reduced by factors of $\sim 10^{13}$ and $\sim 10^{3}$ compared to theoretical values, respectively, and this is attributed to the presence of strain-induced defects. The MQW excitonic absorption coefficient sensitively depends on the carrier density in the QWs, as a result of screening of the electron-hole (e-h) Coulombic interaction. Likewise, ambipolar diffusion is found to depend on the excess carrier density in a nonlinear fashion, as a result of the e-h plasma-induced changes in the local depletion widths in the vicinity of structural defects.

INTRODUCTION

Owing to large nonlinear optical effects, the spatially separated electron-hole (e-h) plasma that can be generated in periodically doped *nipi* multiple quantum well (MQW) structures, exhibits potential for applications in electro-optic devices such as spatial light modulators (SLMs).[1] Because of large enhancements in the excess carrier lifetime and in-plane ambipolar diffusion constant,[2] a large photo-optic modulation of the effective *nipi* bandgap, MQW excitonic absorption, and refractive index can be attained by a relatively weak optical excitation.[1,3] Also, the large control over the plasma density in *nipi*-based SLM structures enables a spatial and quasi-optical modulation of the transmission and reflection of micro/millimeter waves for applications in phased-array signal processing, telecommunication, and radiometry, as recently demonstrated.[4,5] The understanding of the behavior of fundamental MQW-*nipi* parameters, such as excess carrier lifetime τ, ambipolar diffusion coefficient D_a, and excitonic absorption coefficient, α, as a function of excess carrier density is of paramount importance in developing device applications and enhancing the basic understanding of nonlinear electro-optic effects.

The deleterious influence of defects such as misfit dislocations and the associated Cottrell atmosphere of point defects[6] on τ, D_a and α need to be examined when working with strained-layer systems. In particular, the $In_xGa_{1-x}As$/GaAs MQW system, due largely to the transparent nature of the GaAs substrate with respect to the MQW interband transition energies, is a leading candidate for photonic device applications. We have previously demonstrated the feasibility of using a novel technique called *electron beam-induced absorption modulation* (EBIA)[7] to examine the influence of strain-induced defects on τ, D_a and α. In this paper, we have utilized a time-resolved EBIA technique to study the carrier dynamics associated with nonlinear optical phenomena in a *nipi*-doped $In_{0.2}Ga_{0.8}As$/GaAs MQW structure. Based on a phenomenological model, α, D_a, and τ as a function carrier density and the influence of defects therein are

Mat. Res. Soc. Symp. Proc. Vol. 379 © 1995 Materials Research Society

quantitatively analyzed.

EXPERIMENTAL

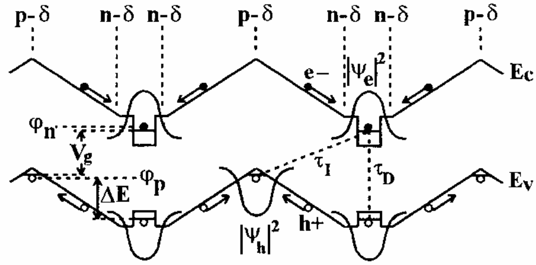

Fig. 1 Band diagram of *nipi*-doped MQWs.

The *nipi*-doped MQW structure was grown by molecular beam epitaxy on a GaAs(001) substrate and consists of 44 $In_{0.2}Ga_{0.8}As$ QWs, each 65 Å thick, and separated by 780-Å-thick GaAs barriers. In the center of each GaAs barrier a *p*-type Be-doping plane with a sheet density of 9.0×10^{12} cm^{-2} was inserted. On both sides of the QWs, using 100 Å thick spacer layers, *n*-type Si-doping planes with a sheet density of 3.0×10^{12} cm^{-2} were inserted. The δ-doping planes induce a linear variation in the band edges along the growth direction as illustrated in Fig. 1. In order to laterally confine the e-h plasma to a well-defined region, conventional lithographic techniques were used to pattern the sample into square mesas of ~90 μm × 90 μm. A non-patterned planar region of ~1 cm × 1 cm was examined to study the effects of defects on the ambipolar diffusion of the e-h plasma. In addition to employing EBIA imaging and spectroscopy techniques as previously reported,[7] we have employed a new *time-resolved* EBIA approach which uses a Boxcar integration technique. The sub-μsec time resolution allows for a measurement of absorption modulation decay behavior, enabling a direct determination of the excess carrier lifetime and diffusion parameters. This complements the sub-μm resolution spatial imaging of $\Delta\alpha$ previously demonstrated with EBIA.[7]

RESULTS AND DISCUSSION

Room temperature EBIA spectra for various electron beam currents, I_b, are shown in Fig. 2 for the planar region. The effective QW absorption coefficients, α, were calculated according to $(-L_{eff})^{-1}\ln T$, where T is the measured normalized transmission through the sample and L_{eff} is the total thickness of the QWs. The peak of the absorption spectrum at ~1005 nm is the n=1 heavy-hole to electron (hh1-e1) excitonic transition. During the continuous generation of e-h pairs by the high-energy (35 keV) electron beam, electrons and holes will be attracted to the QWs and the center of the barriers, respectively, resulting in their spatial separation. Under sufficiently high excitation, the quenching of the hh1-e1 excitonic absorption occurs and is a result of band-filling and screening of the Coulombic interaction of the excitons by the electron plasma filling the QWs. A reliable treatment of screening in semiconductors requires the use of many body theory. For simplicity, however, the screening-induced change in α is often modeled by a simple absorption saturation relationship,[8,10]

$$\alpha = \frac{\alpha_o}{1+\delta n_e/n_{sat}} + \alpha_b, \qquad (1)$$

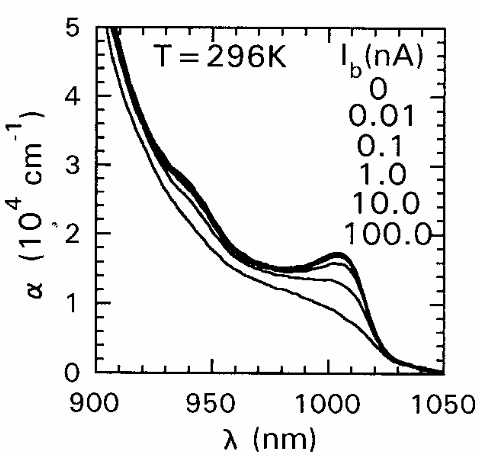

Fig. 2 Absorption spectra at various I_b.

which is a heuristic fitting equation and not based on a theoretically derived model, where δn_e and n_{sat}, respectively, are the two-dimensional excess carrier density and the saturation carrier density, α_b is a band-to-band absorption term, and α_o is the excitonic absorption coefficient in the absence of excitation. The experimental excitonic absorption α as an empirical function of δn_e will be determined from the following phenomenological model, and a deviation from the relationship of Eq. (1) will be discussed.

In the EBIA study here, e-h pairs can be generated nearly uniformly throughout the entire ~3.7 μm MQW region by a 35 keV electron beam.[11] The steady state two dimensional excess carrier density δn_e is given by[1,11]

$$\delta n_e = \frac{\tau P(1-f) I_b}{e E_i A_{ex}} \frac{dE_b}{dz}, \qquad (2)$$

where τ is the lifetime, P is the *nipi* period, dE_b/dz is the electron beam "depth-dose" or energy dissipation function, I_b is the beam current, f is the fractional beam loss due to backscattered electrons (for most cases, $f \ll 1$), e is the electric charge, E_i is the valence electron ionization energy, and A_{ex} is the effective lateral area of excitation. In Eq. (2), A_{ex} for the mesa is ~8100 μm^2, and the only unknown is τ, which can be described according to the phenomenological expression[1,12,13]

$$\tau = \tau_o \exp\left(-\frac{e\beta\delta n_e}{2\varepsilon}\right), \qquad (3)$$

where τ_o and β are parameters which depend on the temperature and the MQW *nipi* structure, and ϵ is the dielectric permittivity of GaAs. Insertion of Eq. (3) into Eq. (2) yields,

$$\delta n_e = \frac{2\varepsilon}{e}\theta I_b exp\left(-\frac{e\beta\delta n_e}{2\varepsilon}\right), \qquad (4)$$

where $\theta=[\tau_o P(dE_b/dz)(1-f)]/(2\epsilon A_{ex} E_i) \approx 4278.8$ kV/cm·nA. Note that from the empirical electron energy loss model of Everhart and Hoff,[11] we estimate that $dE_b/dz \approx 7.53$ keV/μm, and E_i is ~4.8 eV for GaAs. Since τ varies exponentially as a function of δn_e, the recombination rate, which is proportional to the reciprocal of lifetime τ, is no longer a constant when δn_e changes. The time-dependent δn_e in the absence of any carrier generation is given by

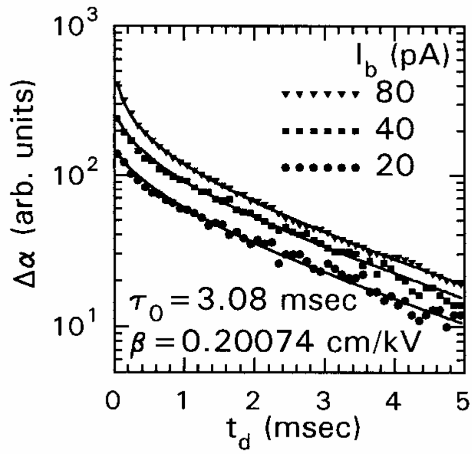

Fig. 3 $\Delta\alpha$ vs. t_d for I_b=20, 40, and 80 pA.

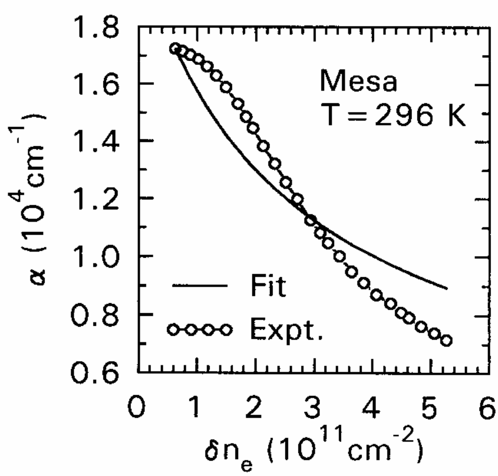

Fig. 4 Experimental and fitted α vs. δn_e curves.

$$\frac{d}{dt}(\delta n_e) + \frac{\delta n_e}{\tau_o \exp[-(e\beta\delta n_e)/(2\varepsilon)]} = 0, \qquad (5)$$

and integration yields

$$\ln(\delta n_e)+\sum_{n=1}^{\infty}\frac{1}{n}\frac{\left[-(e\beta\delta n_e)/(2\varepsilon)\right]^n}{n!}=-\frac{t}{\tau_o}+\Delta;\quad \Delta=\ln(\delta n_o)+\sum_{n=1}^{\infty}\frac{1}{n}\frac{\left[-(e\beta\delta n_o)/(2\varepsilon)\right]^n}{n!}, \tag{6}$$

where δn_o is the initial steady state δn_e in the presence of I_b (i.e., before the electron beam is blanked), and can be determined numerically by Eq. (4), provided β and τ_o are determined. In the limit of weak excitation, the differential excitonic absorption $\Delta\alpha$ to a first order of approximation, is proportional to δn_e, according to Eq. (1). The experimental data of $\Delta\alpha$ vs. t_d (the time delay after a steady-state excitation) at various I_b are shown in Fig. 3. The solid curves are the results of a nonlinear least square fit of this data at I_b=20, 40, and 80 pA simultaneously to Eq. (6), yielding β=0.20074 cm/kV and τ_o=3.08 msec. Note that a further increase of I_b results in a gradual deviation of β due to a deviation from the linear relationship between δn_e and $\Delta\alpha$, which prevails only at weak excitation ($I_b \lesssim 100$ pA). Inserting the value of β and τ_o into Eq. (4), therefore, allows for a determination of δn_e for various I_b. The experimental results of α vs. δn_e and a fit to the model of Eq. (1) are shown in Fig. 4. The fit gives n_{sat}=2.5x10^{11} cm^{-2}, consistent with previous estimates of n_{sat}.[8,14] The quenching of α is found to be more rapid than that described by Eq. (1) when $\delta n_e \gtrsim 1.5\times10^{11}$ cm^{-2}. The observed large deviation between the α vs. δn_e curve and the fit of Eq. (1) in Fig. 4 is attributed to an absence of a treatment of screening in the model of Eq. (1) which, as we show, should only be used as a rough approximation.

Using Eq. (3), the data of Fig. 4, and the aforementioned values of β and τ_o, the relationships of δn_e and τ as a function of I_b in the planar region can be determined and are shown in Fig. 5. We have previously shown that, in another *nipi*-doped MQW structure under a weak excitation, a nearly 9 orders of magnitude reduction of τ_o as compared to a theoretically calculated lifetime, τ_{th}, is attributed to the presence of defects which provide additional recombination channels.[13] Similarly, τ_o here is ~10^{13} less than the τ_{th} calculated by Jonsson *et al.*[14] for an effective *nipi* barrier height of 1.257 eV for this nominal structure. Such a reduction in lifetime confirms the effect of structural defects on increasing the recombination rate of excess carriers.

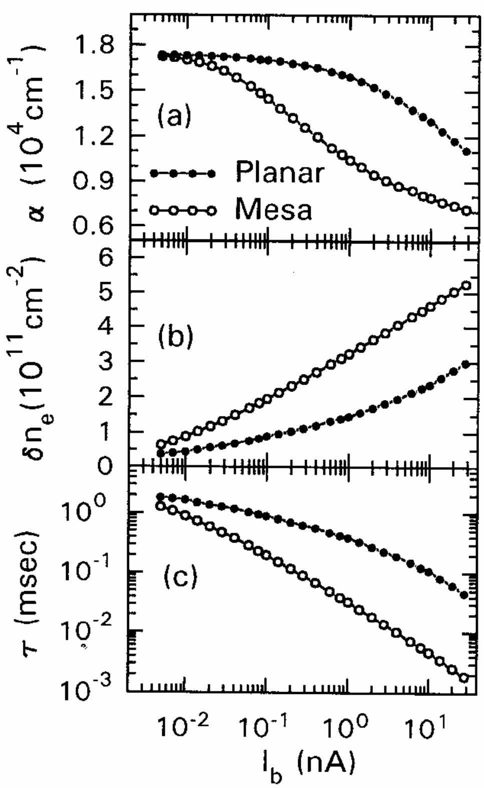

Fig. 5 Experimental results of (a) α, and phenomenologically derived (b) δn_e, and (c) τ as a function of I_b.

The model of Eq. (4) can be applied to the planar region, provided a few modifications are made to account for the variation in A_{ex}. In contrast to the confined mesa region, A_{ex} is equal to πL_D^2 and the diffusion length L_D is excitation dependent[1,7,12] for the planar region. The parameter θ is thus excitation dependent in the planar region and can be written as

$$\theta=\kappa(\pi L_D^2)^{-1}, \tag{7}$$

where κ is excitation independent and κ=0.3466 kV·cm/nA, as obtained from $\theta\cdot A_{ex}$ for the mesa. Substitution of Eq. (7) into Eq. (4) with the results of δn_e vs. I_b shown in Fig. 5(b) allows for the determination of L_D and D_a ($=L_D^2/\tau$) as a function of δn_e, as shown in Figs. 6(a) and 6(b), respectively. A theoretical expression for D_a (designated as D_{th}) has been derived by Gulden *et al.*[15] and is

$$D_{th} = \frac{1}{e^2}\frac{\sigma_n \sigma_p}{\sigma_n + \sigma_p}\frac{\partial \phi_{np}}{\partial n}, \quad (8)$$

where $\sigma_n = ne\mu_n$ and $\sigma_p = pe\mu_p$ are the *n*- and *p*-layer conductivities, *n* and *p* are the average 3-dimensional excess carrier densities which are given by $\delta n_e/P$ and $\delta n_h/P$, respectively, and $\phi_{np} = \phi_n - \phi_p$ is the difference in quasi-Fermi levels. The 2D excess hole density, δn_h, is given by $\delta n_h \approx \delta n_e + \delta N_A$, since most of the dopants are ionized at room temperature. An excess δ-*p* doping concentration of $\delta N_A = 3.0\times10^{12}$ cm^{-2}, relative to δ-*n* doping, was inserted in order to locate the Fermi-level sufficiently far below the electron ground state in the QWs to ensure that the QWs are essentially free from electrons under thermal equilibrium. The lower limit for the ideal mobilities μ_n and μ_p are estimated to be ~3100 and ~170 cm^2/v·s, respectively, for equivalent 3-dimensional doping densities in GaAs.[16] For the present δ-doped *nipi* structure, $\partial\phi_{np}/\partial n$ is approximately a constant[15] and is given by $\partial\phi_{np}/\partial n = (eP)^2/4\epsilon$. The theoretical diffusion coefficient, D_{th}, versus δn_e is plotted in Fig. 6(b). The experimental values for D_a are observed to lie nearly 3 orders of magnitude below D_{th} for $\delta n_e \leq 0.5\times10^{11}$ cm^{-2}, and gradually increase to within ~20% of D_{th} for $\delta n_e \geq 3.0\times10^{11}$ cm^{-2}. In a previous study,[7,13] it was shown that the reduction of D_a was caused by strain-induced defects which create potential fluctuations that increase scattering of mobile carriers. The reduction in discrepancy between D_a and D_{th} for higher carrier concentration was not observed in the study of Ref. 12 since only very low carrier concentrations were examined. It is our hypothesis that the convergence of D_a and D_{th} for higher concentrations is related to changes in the local depletion width surrounding point defects and misfit dislocations in the MQW. These defects can create a local density of midgap states that will force the Fermi levels (and quasi-Fermi levels under excitation) to reside closer to mid-gap, inducing a repulsive barrier that impedes carrier motion. The latter effect also gives rise to the repulsion of majority carries from the edge of a cleaved *nipi* sample. Each defect will cause a 3-D depletion region whose complex shape will depend on the local doping density and carrier concentration. The increase in local carrier concentration caused by the excitation will reduce the size of the depletion region and reduce the magnitude of the potential fluctuations by screening the charge associated with the defects. The effective reduction in scattering cross-section at higher excess carrier concentrations will consequently result in an increased D_a, as experimentally observed.

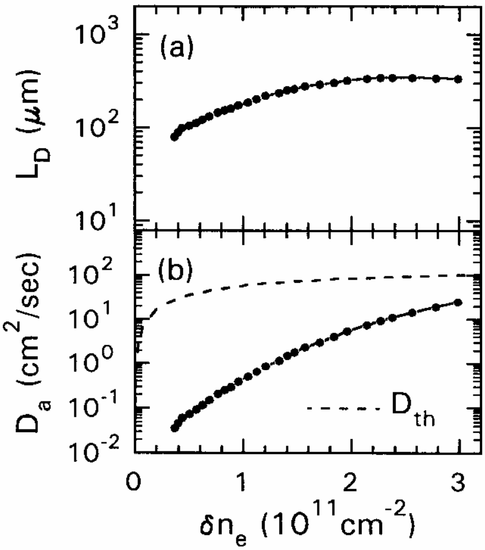

Fig. 6 (a) Diffusion length L_D, and (b) ambipolar diffusion coefficient D_a as a function of δn_e.

CONCLUSION

In conclusion, the modulation of MQW exciton absorption has been studied with the use of a novel time-resolved EBIA technique. The excess carrier lifetime and ambipolar diffusion coefficient are found to be reduced by factors of ~10^{13} and ~10^3, respectively, relative to theoretical values for the low excitation densities. This reduction is attributed to the strain-induced misfit dislocations and point defects. A more rapid decrease of α for high carrier densities than that predicted by the conventional absorption satuation relationship suggests that a more sophisticated model which incorporates the effect of screening needs to be developed. The experimentally determined ambipolar diffusion coefficient, D_a, is found to approach its theoretical estimate, D_{th}, as the carrier density is increased. This phenomenon is suggested to be caused by a reduction in (*i*) the size of defect-induced depletion regions and (*ii*) the height of band-edge potential fluctuations for increased carrier densities.

ACKNOWLEDGEMENTS

This work was sponsored by the U.S. Army Research Office and the National Science Foundation.

REFERENCES

1. J. Maserjian, P.O. Andersson, B.R. Hancock, J.M. Iannelli, S.T. Eng, F.J. Grunthaner, K.-K. Law, P.O. Holtz, R.J. Simes, L.A. Coldren, A. C. Gossard, and J.L. Merz, Appl. Opt. **28**, 4801 (1989).
2. K.H. Gulden, H. Lin, P. Kiesel, P. Riel, G.H. Döhler, and K.J. Ebeling, Phys. Rev. Lett. **66**, 373 (1991).
3. G.H. Döhler, IEEE J. Quantum Electron. **QE-22**, 1682 (1986); J. Vac. Sci. Technol. **B 1**, 278 (1983).
4. A. Kost, L. West, T.C. Hasenberg, J.O. White, M. Matloubian, and G.C. Valley, Appl. Phys. Lett. **63,** 3494-3496 (1993).
5. G. Delgado, J. Johansson, A. Larsson, and T. Andersson, *Optically controlled spatial modulation of (sub-) millimeter waves using nipi-doped semiconductors*, 1994 (unpublished).
6. D.H. Rich, K.C. Rajkumar, L. Chen, A. Madhukar, T. George, J. Maserjian, F.J. Grunthaner, and A. Larsson, J. Vac. Sci. Technol. **B 10**, 1965 (1992).
7. D.H. Rich, K. Rammohan, Y. Tang, H.T. Lin, J. Maserjian, F.J. Grunthaner, A. Larsson, and S.I. Borenstain, Appl. Phys. Lett. **63**, 394 (1993); J. Vac. Sci. Technol. **B 11**, 1717 (1993); Appl. Phys. Lett. **64**, 730 (1994).
8. S.H. Park, J.F. Morhange, A.D. Jeffery, R.A. Morgan, A. Chavez-Pirson, H.M. Gibbs, S.W. Koch, N. Peyghambarian, M. Derstine, A.C. Gossard, J.H. English, and W. Weigmann, Appl. Phys. Lett. **52**, 1201 (1988).
9. D.S. Chemla, D.A.B. Miller, P.W. Smith, A.C. Gossard, and W. Wiegmann, IEEE J. Quantum Electron. **QE-20**, 265 (1984).
10. M. Kawase, E. Garmire, H.C. Lee, and P.D. Dapkus, IEEE J. Quantum Electron. **QE-30**, 981 (1994).
11. T.E. Everhart and P.H. Hoff, J. Appl. Phys. **42**, 5837 (1971).
12. J.M. Iannelli, J. Maserjian, B.R. Hancock, P.O. Andersson, and F.J. Grunthaner, Appl. Phys. Lett. **54**, 301 (1989).
13. D.H. Rich, H.T. Lin, and A. Larsson, J. Appl. Phys, in press.
14. B. Jonsson, A.G. Larsson, O. Sjölund, S. Wang, T.G. Andersson, and J. Maserjian, IEEE J. Quantum Electron. **QE-30**, 63 (1994).
15. K.H. Gulden, H. Lin, P. Kiesel, P. Riel, G.H. Döhler, K.J. Ebeling, Phys. Rev. Lett. **66**, 373 (1991).
16. S.M. Sze, Physics of Semiconductor Devices, 2nd ed. (Wiley, New York, 1981), p. 29.